URSI GASS 2021, Rome, Italy, 28 August - 4 September 2021

Multiscale Porous Elastomer Substrate Enabled Harmonic Face Mask for Wireless Cough Monitoring

Liang Zhu*(1) and Pai-Yen Chen(1)
(1) Department of Electrical and Computer Engineering, University of Illinois at Chicago, Chicago, IL 60607, USA

Abstract

In this paper, we propose and experimentally demonstrate a wireless smart face mask based on a passive harmonic tag for real-time cough monitoring. The proposed harmonic mask is fabricated on multiscale porous polystyrene blockpoly (ethylene-ran-butylene) block polystyrene (SEBS) supporting substrates, thereby achieving several advantages including passive-cooling functionality, high breathability and outstanding waterproofing. Our results show that by applying this on-mask electronics, the cough event can be successfully monitored through non-contact track of the received signal strength indicator (RSSI) at the harmonic frequency. Moreover, compared to the conventional backscatter RFID detector vulnerable to environmental noise, the harmonic tag-based smart mask can well suppress the electromagnetic interferences, such as clutters and crosstalks, thanks to the frequency orthogonality between the launched and backscattered radio-frequency (RF) signals. We envision that this zero-power and lightweight wearable electronics could be beneficial for cough monitoring and the public health condition tracking, and may pave the way for widespread applications such as next-generation smart textiles.

1 Introduction

Cough, which is a common symptom in many respiratory diseases including pneumonia and tuberculosis, may appear sporadically with colds or flu to act as a protective mechanism, but when it becomes chronic, it could severely impair life quality by interfering with normal daily activities, for example, breathing or sleeping [1, 2]. As a result, this symptom is the commonest reason for people seeking medical advice, and the assessment of cough frequency is considered as a critical tool in clinical use. To date, various emerging cough monitoring platforms have been developed [3], which could be divided into three categories. The first one depends on the airflow measurement, which requires placing detection module (e.g., piezoelectric sensor) close to the nose or mouth to obtain the flow dynamics of cough [4]. However, this method is clearly not suitable for continuous cough monitoring in the outpatient environment [4]. The second type is based on monitoring the movement of the chest or abdominal wall [5], which requires an accelerometer directly placed at the volunteer's chest wall to record cough

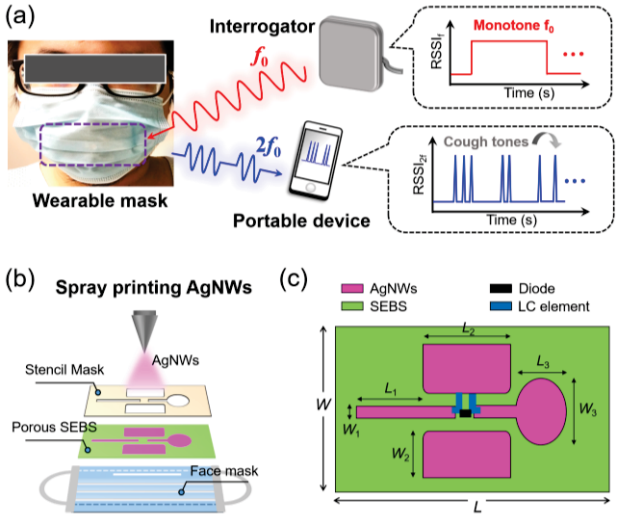

Fig. 1. (a) Schematics of the smart face mask based on a passive, lightweight, and low-profile harmonic tag. (b) A schematic diagram of the spray printing of AgNWs onto prestretched porous SEBS through a stencil mask. (c) Geometry of the harmonic tag embedded in the face mask.

events. Hence, a trained operator is demanded to manually identify cough events, which is a rather time- consuming and arduous task [5]. The third one relying on the measurement of cough sounds has been more universal with the advent of computer technology and the availability of portable digital sound recording devices [6]. Unfortunately, these automatic cough monitors typically suffer from confusion with surrounding noises and other parasitic patient sounds (e.g., throat clearing, humming, or laughing) that are not associated with the disease transmissive event.

In the last decades, radio-frequency (RF) approaches have been explored for remotely detecting and monitoring cough events [7], primarily focusing on the designs of antenna sensors and passive radio frequency identification (RFID). However, it is well known that these backscattering tags are usually vulnerable to a low signal-to-clutter/noise ratio in noisy indoor environments, which impedes the real-time, continuous and accurate monitoring of coughs. Inspired by this demand, the harmonic transponder sensor (or harmonic sensor) has been recently proposed with the received and transmitted RF signals orthogonal to each other (e.g., fundamental frequency and harmonics), thereby avoiding multipath interferences, clutters, and crosstalks [8-10].

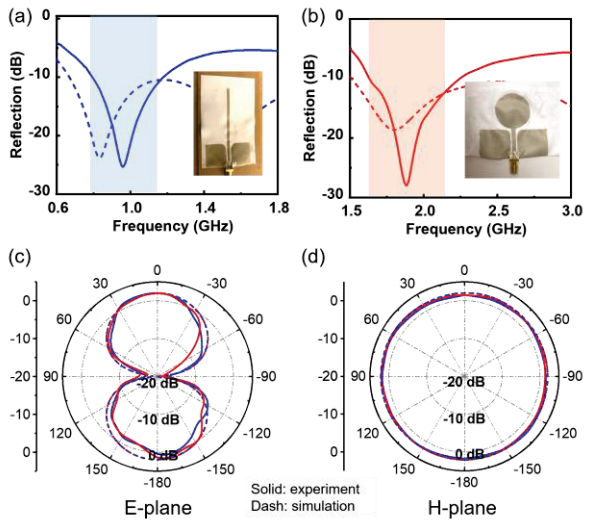

Fig. 2. Measured (solid line) and simulated (dashed line) reflection coefficient versus frequency for (a) rectangular monopole and (b) circular monopole antennas, with their measured (solid line) and simulated (dashed) radiation patterns in (c) and (d) on the E-plane and H-plane, respectively.

Although harmonic sensors have been used in remote sensing of mechanical cracks [11], liquid levels [12], and biochemical processes [13], as well as localization of underground buried assets [14], their substrate and metal layer are still limited to printed circuit board (PCB) and copper strips, which pose a challenge in future applications including wearable or on-skin electronics.

In this work, we propose a lightweight harmonic sensor made by silver nanowires (AgNWs) and multiscale porous elastomer substrate (SEBS) that can be flawlessly embedded in the face mask to perform rapid, real-time wireless cough monitoring. The schematic of the harmonic mask is sketched in Fig. 1(a). In the following, we will detail the antenna and frequency multiplier designs, the sensing mechanism and conducting a real-time cough event monitoring in noisy indoor environment.

2 Antenna designs and measurement

Fig. 1(b) depicts the fabrication process of the proposed harmonic mask, which consists of a harmonic transponder created by spraying printing of the AgNWs onto SEBS and attached to a typical face mask. Here, AgNWs (diameter, 50 nm; length, 100 to 200 μm) are used mainly because they exhibit outstanding mechanical compliance and high electrical conductivity (~200 nm thick with conductivity 11,000 S/cm), and can be easily produced in a large quantity. Moreover, the SEBS elastomer is adopted mainly due to its high stretchability and breathability, excellent biocompatibility and solution processability, making it well suitable for wearable or on-skin electronics. Fig. 1(c) illustrates the top view of the proposed harmonic transponder comprising two monopole antennas and a frequency multiplier formed by lumping elements. The designed parameter is summarized as: $L = 55$, $W = 30$, $L_1 = 15$, $L_2 = 15$, $L_3 = 10$, $W_1 = 2.5$, $W_2 = 6.5$, $W_3 = 8.5$, with the unit mm. The two microstrip antennas are matched to a 50 Ω coplanar waveguide (CPW), and both fabricated on the flexible SEBS substrate with relative permittivity $\varepsilon_r = 2.6$, loss tangent $\delta = 0.04$, and thickness of only 0.2 mm. Figs. 2(a) and 2(b) report the measured reflection coefficient (S_{11}) and photographs for the monopole antennas. It can be seen that the rectangular monopole antenna resonates at 0.9 GHz (fundamental frequency) with a -10 dB bandwidth of 354 MHz, while the elliptical one works at the second-harmonic frequency (1.8 GHz) with a -10 dB bandwidth of 521 MHz. Figs. 2(c) and 2(d) reports the radiation patterns of the monopole antennas at their resonant frequencies. We find that the measured radiation patterns agree well with the simulated ones on both E-plane and H-plane. In addition, the antennas both exhibit an omnidirectional radiation property, with the maximum measured gain of 2.11 dBi at 0.9 GHz for rectangular monopole and 2.45 dBi at 1.8 GHz for the elliptical one. Both antennas have the radiation efficiency greater than 85 % at the resonant frequency.

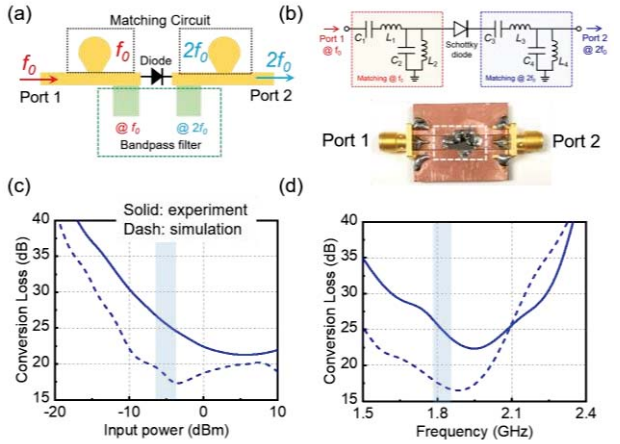

Fig. 3. (a) Circuit schematic and (b) implementation of a lumping element based frequency multiplier, and its simulated and measured conversion loss in (c) as a function of input power and in (d) at different output frequency.

These antennas are integrated with a passive frequency multiplier [Fig. 3] for building a passive harmonic transponder. The schematic diagram and photograph of the passive frequency multiplier are presented in Figs. 3(a) and 3(b), whose input and output ports are connected to two monopole antennas. Here, we built the bandpass filters and matching networks with lumped elements and a Schottky diode (SMS 7621) to reduce area occupation of the harmonic tag, with the design parameters concluded as: $C_1 = 10$, $L_1 = 22$, $C_2 = 3.3$, $L_2 = 3.9$, $C_3 = 3.6$, $L_3 = 2$, $C_4 = 22$, $L_4 = 36$; here, the unit for capacitors (inductors) is pF (nH). The passbands of the *LC* band-pass filters on the input and output sides are centered at 0.9 GHz and 1.8 GHz, respectively. Fig. 3(c) reports the conversion loss of the passive frequency multiplier at 0.9 GHz, in response to different input power. It can be observed that at the 0 dBm input level, a conversion loss ~25.3 dB could be achieved. Fig. 3(d) reports the measurement results for the conversion loss versus the second-harmonic frequency at

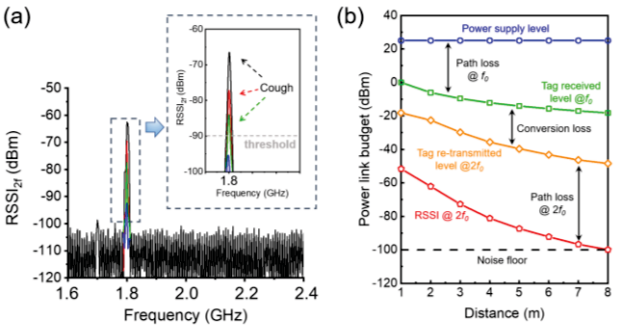

Fig. 4. (a) Measured RSSI with the existence of cough at different interrogating distance (black: 2m; red: 3m; green: 4m; blue: 6m), in which the interrogating signal is an unmodulated CW carrier at 0.9 GHz. (b) Calculated power link and measured received power when the proposed transponder is placed in a distance range from 1 to 8 m.

input power of -5 dBm. The frequency dependency shows that the minimum conversion loss (~22.5 dB) was obtained at 1.95 GHz.

After testing these components, the afore-studied antennas and frequency multiplier were spray printed together on SEBS substrate to make a flexible harmonic transponder [Figs. 1(b) and 1(c)]. Hereafter, this compact, low-profile passive harmonic tag was adhered to a typical face mask and a protection layer to form a harmonic mask for wireless cough monitoring applications [Fig. 1(a)].

3 Harmonic mask for cough monitoring

To test this harmonic mask, we adopted the bistatic measurement setup in a cluttered indoor environment. During the measurement, the reader's transceiver continuously launches an CW interrogation signal (at 0.9 GHz) to the user wearing the harmonic mask. The frequency and pattern of cough can be obtained from the recorded time series of the second-harmonic RSSI (at 1.8 GHz). The sensing mechanism could be understood as follow. According to the Friis transmission equation, the second-harmonic RSSI (i.e., received power P_r) can be estimated as [15]:

$$\frac{P_r}{P_t} = \left(\frac{\lambda_0}{4\pi R_1}\right)^2 \times \left(\frac{\lambda_0/2}{4\pi R_2}\right)^2 \times \frac{G_r G_t G_R G_T}{L_{sys}} \qquad (1)$$

where G_r is the realized gain of the rectangular monopole antenna at f_0, G_t is the realized gain of the elliptical monopole antenna at $2f_0$, G_T (G_R) denote the realized gain of the reader's transmitter (sniffer), R_1 (R_2) is the distance between reader (sniffer) and the face mask, L_{sys} is the overall system loss including the conversion loss of the frequency multiplier and the insertion loss in filters, transmission line and cables. Some important parameters include: $P_t = 20$ dBm, $R_1 = R_2 = 1.5$ m, $G_T = 11.5$ dBi at 0.9 GHz, and $G_R = 14.0$ dBi at 1.8 GHz. From Eq. (1), it is evident that under a fixed transmitted power P_t, the received power P_r is proportional to the realized gain G_r and G_t of the antennas, which is sensitive to the occurrence of cough. In principle, when the user wearing the harmonic

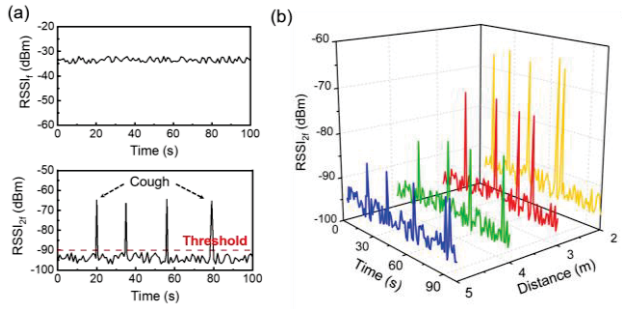

Fig. 5. (a) Measured time series of conventional backscatter $RSSI_f$ (top) and harmonic $RSSI_{2f}$ (bottom) at an interrogating distance of 2.0 m, (b) Measured harmonic $RSSI_{2f}$ at different distance ranging from 1 to 4 m.

mask is at rest (which corresponds to the OFF state of the harmonic tag), the face mask is in close contact with or the proximity of mouth (i.e., air gap g ~ 0) such that the dielectric loading effect of human tissues will shift the resonant frequencies of the antennas and, consequently, the resonant frequencies of antennas do not match to 0.9 GHz and 1.8 GHz, leading to a very small G_r and G_t, and thus low harmonic RSSI. On the other hand, when cough happens, the effect of human body disappears (i.e., g > 10 mm) and the RF monotone can be received by the antenna on the face mask, undergoing the frequency multiplication process ($f_0 \rightarrow 2f_0$), and being re-transmitted to the reader or sniffer. In this case, the harmonic tag can be waked up (i.e., ON state) due to coughs, whose frequency and pattern can be retrieved from the time series of the RSSI at the second-harmonic frequency [Fig. 4(a)]. In other words, the occurrence of cough can dynamically reconfigure the resonant frequencies of the monopole antennas back to 0.9 GHz and 1.8 GHz. As a result, the cough events can be continuously monitored by analyzing the harmonic RSSI pattern over time.

Finally, we validate robustness and effectiveness of our platform by performing the real-time cough monitoring in the noisy environment. The harmonic RSSI is recorded over 100 s. The results reported in Fig. 5(b) shows that the proposed smart face mask enables robust, accurate, and real-time cough monitoring. Fig. 5(c) presents the measured time series of the second-harmonic RSSI at different interrogation distances; here, except for the tag-to-sniffer distance (R_2), all the other measurement conditions remain the same. It is evidently seen that the pattern of transient response of the smart face mask remains unchanged, regardless of the interrogation distance. Therefore, we conclude that the proposed wearable device may provide an accurate cough monitoring with excellent robustness and reliability. For a comparison, we also employed the traditional passive antenna sensor to wirelessly monitor the same cough event. This antenna sensor consists of a microstrip monopole antenna terminated by a 50 Ω match load. The measured variations of RSSI at 0.9 GHz is presented in Fig. 5(a). Apparently, although the RSSI is still modulated over time, the measured backscattered signal cannot be differentiated from the background noises sourced mainly from

crosstalks and clutters.

4 Conclusion

In this paper, we have demonstrated a lightweight, low-profile and fully-passive harmonic tag embedded in a face mask for the continuous, real-time wireless cough monitoring. Specifically, the metal strips are spray printed of silver nanowires and the substrate is formed by porous SEBS elastomer. In the scheme of harmonics-based sensing, the proposed wearable sensor is capable of measuring the frequency and pattern of cough in the far zone of the cluttered indoor environment, and at the same time maintaining high stretchability and breathability, excellent biocompatibility and solution processability. Moreover, comparing to traditional cough monitoring approaches based on passive antenna sensors or backscatter RFIDs, the proposed smart face mask could offer much improved accuracy, robustness, and reliability in real-life applications, potentially benefiting the rapid healthcare tests (e.g., point-of-care testing and driver through tests), telemedicine, healthcare internet-of-things, and biomedical and clinical research.

5 References

[1] K. F. Chung, "Methods of assessing cough and antitussives in man," *Pulmonary Pharmacology & Therapeutics,* vol. 9, no. 5-6, pp. 373-377, Oct-Dec 1996.

[2] R. S. Irwin, F. J. Curley, and C. L. French, "The spectrum and frequency of causes, key components of the diagnostic evaluation, and outcome of specific therapy," *American Review of Respiratory Disease,* vol. 141, no. 3, pp. 640-647, Mar 1990.

[3] C. Z. Li, V. M. Lubecke, O. Boric-Lubecke, and J. S. Lin, "A review on recent advances in doppler radar sensors for noncontact healthcare monitoring," *Ieee Transactions on Microwave Theory and Techniques,* vol. 61, no. 5, pp. 2046-2060, May 2013.

[4] W. T. Goldsmith, A. M. Mahmoud, J. S. Reynolds, W. G. McKinney, A. A. Afshari, A. A. Abaza *et al.*, "A system for recording high fidelity cough sound and airflow characteristics," *Annals of Biomedical Engineering,* vol. 38, no. 2, pp. 469-477, Feb 2010.

[5] Y. T. Hu, E. G. Kim, G. Cao, S. Liu, and Y. Xu, "Physiological acoustic sensing based on accelerometers: A survey for mobile healthcare," *Annals of Biomedical Engineering,* vol. 42, no. 11, pp. 2264-2277, Nov 2014.

[6] P. Munyard, C. Busst, R. Logansinclair, and A. Bush, "A new device for ambulatory cough recording," *Pediatric Pulmonology,* vol. 18, no. 3, pp. 178-186, Sep 1994.

[7] P. Sharma, X. N. Hui, and E. C. Kan, "A wearable rf sensor for monitoring respiratory patterns," *2019 41st Annual International Conference of the Ieee Engineering in Medicine and Biology Society (Embc),* pp. 1217-1223, 2019.

[8] L. Zhu, N. Alkhaldi, H. M. Kadry, S. Liao, and P. Y. Chen, "A compact hybrid-fed microstrip antenna for harmonics-based radar and sensor systems," *Ieee Antennas and Wireless Propagation Letters,* vol. 17, no. 12, pp. 2444-2448, Dec 2018.

[9] X. Gu, N. S. Nikhil, L. Guo, S. Hemour, and K. Wu, "Diplexer-based fully passive harmonic transponder for sub-6-ghz 5g-compatible iot applications," *Ieee Transactions on Microwave Theory and Techniques,* vol. 67, no. 5, pp. 1675-1687, May 2019.

[10] J. R. Riley, A. D. Smith, D. R. Reynolds, A. S. Edwards, J. L. Osborne, I. H. Williams *et al.*, "Tracking bees with harmonic radar," *Nature,* vol. 379, no. 6560, pp. 29-30, Jan 4 1996.

[11] D. Ahbe, S. Beer, T. Zwick, Y. Wang, and M. M. Tentzeris, "Dual-band antennas for frequency-doubler-based wireless strain sensing," *Ieee Antennas and Wireless Propagation Letters,* vol. 11, pp. 216-219, 2012.

[12] H. Y. Huang, P. Y. Chen, C. H. Hung, R. Gharpurey, and D. Akinwande, "A zero power harmonic transponder sensor for ubiquitous wireless mu l liquid-volume monitoring," *Scientific Reports,* vol. 6, Jan 6 2016.

[13] L. Zhu, H. Y. Huang, M. M. C. Cheng, and P. Y. Chen, "Compact, flexible harmonic transponder sensor with multiplexed sensing capabilities for rapid, contactless microfluidic diagnosis," *Ieee Transactions on Microwave Theory and Techniques,* vol. 68, no. 11, pp. 4846-4854, Nov 2020.

[14] A. Abdelnour, A. Lazaro, R. Villarino, D. Kaddour, S. Tedjini, and D. Girbau, "Passive harmonic rfid system for buried assets localization," *Sensors,* vol. 18, no. 11, Nov 2018.

[15] J. A. Shaw, "Radiometry and the friis transmission equation," *American Journal of Physics,* vol. 81, no. 1, pp. 33-37, Jan 2013.